Oncogene (2008) 27, 4690–4701

www.nature.com/onc

ORIGINAL ARTICLE

Snai1 and Snai2 collaborate on tumor growth and metastasis properties of mouse skin carcinoma cell lines

D Olmeda[1,3], A Montes[1], G Moreno-Bueno[1], JM Flores[2], F Portillo[1] and A Cano[1]

[1]*Departamento de Bioquímica, UAM, Instituto de Investigaciones Biomédicas 'Alberto Sols' CSIC-UAM, Madrid, Spain and* [2]*Departamento de Cirugía y Medicina Animal, Facultad de Veterinaria, UCM, Madrid, Spain*

Snai1 (Snail) and Snai2 (Slug), the two main members of Snail family factors, are important mediators of epithelial-mesenchymal transitions and involved in tumor progression. We recently reported that Snai1 plays a major role in tumor growth, invasion and metastasis, but the contribution of Snai2 to tumorigenesis is not yet well understood. To approach this question we have silenced Snai2 and/or Snai1 by stable RNA interference in two independent mouse skin carcinoma (HaCa4 and CarB) cell lines. We demonstrate that Snai2 knockdown has a milder effect, but collaborates with Snai1 silencing in reduction of tumor growth potential of either carcinoma cell line when injected into nude mice. Importantly, Snai1 or Snai2 silencing dramatically influences the metastatic ability of squamous carcinoma HaCa4 cells, inducing a strong reduction in liver and lung distant metastasis. However, only Snai1 knockdown has an effective action on invasiveness and fully abolishes tumor cell dissemination into the spleen. These results demonstrate that Snai1 and Snai2 collaborate on primary tumor growth and specifically contribute to site-specific metastasis of HaCa4 cells. These data also indicate that Snai1 is the major regulator of local invasion, supporting a hierarchical participation of both factors in the metastatic process.
Oncogene (2008) **27,** 4690–4701; doi:10.1038/onc.2008.118; published online 14 April 2008

Keywords: Snai1; Snai2; E-cadherin; EMT; invasion; metastasis

Introduction

Despite the enormous knowledge accumulated in the past decades on the mechanisms of tumor generation, very little is still known about the molecular mechanisms governing metastatic dissemination (Mehlen and Puisieux, 2006). Local invasion is presently considered as the leading event for carcinoma metastasis (Christofori, 2006; Gupta and Massague, 2006). During the invasive process, tumor cells lose their cell–cell adhesion properties and undergo profound changes in their phenotype known as epithelial-mesenchymal transition (EMT), a process reminiscent of developmental EMT (Nieto, 2002; Thiery, 2002). Downregulation of E-cadherin is a hallmark of EMT and occurs frequently during carcinoma progression (Birchmeier and Behrens, 1994; Christofori and Semb, 1999; Thiery, 2002). Transcriptional repression mechanisms of *E-cadherin* have been intensively investigated in the last years and several transcription factors characterized as *E-cadherin* repressors (reviewed in Peinado *et al*., 2007). Among them, two members of the Snail superfamily, Snai1 (Snail; Batlle *et al*., 2000; Cano *et al*., 2000) and Snai2 (Slug; Hajra *et al*., 2002; Bolos *et al*., 2003) are presently considered key regulators of EMT (Nieto, 2002). Although the function of Snai1 and Snai2 can be interchangeable in different species (Barrallo-Gimeno and Nieto, 2005), a distinct role for each factor is supported from analysis of knockout mice. While *Snai1* null mice present early embryonic lethality (Carver *et al*., 2001), *Snai2* null mice are viable, undergoing a normal program of development (Jiang *et al*., 1998). The specific contribution of Snai1 and Snai2 to tumor progression is still poorly defined. Recent studies on Snail factors indicate that either Snai1 and/or Snai2 can be expressed in different carcinomas, including breast, ovarian, colon and squamous cell carcinomas, sometimes associated to invasion, metastasis and/or poor prognosis (Peinado *et al*., 2007). Previous studies on human breast carcinoma cells also suggested a differential involvement of Snai1 and Snai2 in *E-cadherin* repression or specific invasion patterns (Hajra *et al*., 2002; Come *et al*., 2006). We recently described an important role for Snai1 in tumor growth, differentiation and invasion of mouse skin (Olmeda *et al*., 2007a), and in lymph node metastasis of human breast carcinoma cells (Olmeda *et al*, 2007b). Now, we have investigated the interplay between Snai1 and Snai2 in tumorigenesis targeting each factor by stable RNA interference in two mouse skin carcinoma cell lines, analysing their effect in *in vitro* invasion, and tumorigenic and metastatic behaviour into nude mice. Our results indicate that Snai1 and Snai2 collaborate on

Correspondence: Dr A Cano, Department of Biochemistry, UAM, Instituto de Investigaciones Biomédicas 'Alberto Sols' CSIC-UAM, c/Arturo Duperier 4, Madrid 28029, Spain.
E-mail: acano@iib.uam.es
[3]Current address: Centro Nacional de Investigaciones Oncológicas, Melchor Fernández Almagro, Madrid, Spain.
Received 5 September 2007; revised 6 February 2008; accepted 7 March 2008; published online 14 April 2008

in vivo tumor growth and induction of lung and liver distant metastasis. Importantly, Snai1 is determinant for local invasion and tumor cell dissemination into spleen. Together, these data support an interplay and hierarchical participation of Snai1 and Snai2 during tumor progression.

Results

shSnai2 inhibits Snai2 expression without affecting Snai1
We have previously reported that Snai2 represses the proximal *E-cadherin* promoter inducing a full EMT process (Bolos *et al*., 2003). We first used MDCK-Snai2 cells to prove that siRNA against *Snai2* abrogates its transcriptional repression, by choosing a 19-mer C-terminal *Snai2* sequence not present in *Snai1* mRNA of any species (Manzanares *et al*., 2001), cloned into pTER-Zeo vector. The shSnai2 derepressed *E-cadherin* promoter in MDCK-Snai2 cells in a dose-dependent manner (Supplementary Figure S1A). It also blocked the repressive action of Snai2-EGFP in MDCK cells. Importantly, the effect of shSnai2 is specific as it did not influence Snai1-EGFP mediated repression of *E-cadherin* promoter (Supplementary Figure S1B). As previously reported, shSnai1 is specific for Snail1 repression (Supplementary Figure S1B; Olmeda *et al*., 2007a).

Interference of endogenous Snai2 in carcinoma cells affects EMT markers and cooperates with Snai1 silencing in decreased invasiveness
The effectiveness of shSnai2 to block endogenous Snai2 expression was analysed in two mouse epidermal carcinoma cell lines, derived from mouse squamous cell carcinoma (HaCa4) and spindle cell carcinoma (CarB), extensively characterized previously as E-cadherin deficient, expressing high levels of Snai1 and Snai2, and showing highly invasive, tumorigenic and metastatic behaviour (Navarro *et al*., 1991; Llorens *et al*., 1998; Cano *et al*., 2000). We have recently reported that endogenous Snai1 silencing in HaCa4 and CarB cells leads to decreased expression of mesenchymal markers and invasiveness (Olmeda *et al*., 2007a). To answer whether Snai2 could collaborate with Snai1 in the phenotype and tumorigenic behaviour of both carcinoma cell lines, the shSnai2 vector was stably transfected in HaCa4 and CarB cells in the absence or presence of shSnai1. Stable clones (5–10) were isolated and characterized from each cell line and transfection (named HaCa4-shSnai2 or CarB-shSnai2 for shSnai2, and HSS and CSS for shSnai1/shSnai2 double interference); two representative examples of each type are shown. Two selected clones of the recently described HaCa4-shSnai1 and CarB-shSnai1 cells (Olmeda *et al*., 2007a) were included. Cells stably transfected with shEGFP (HaCa4-shEGFP and CarB-shEGFP) were used as negative controls. Reverse transcription (RT)–PCR and immunoblot analyses showed the effectiveness of Snai2 and/or Snai1 silencing (Figures 1a and b, and data not shown), demonstrating the almost total blockade of Snai2 and/or Snai1 expression. The specificity of the individual interference was also evidenced; no significant changes in endogenous Snai1 or Snai2 levels were detected in the shSnai2- and shSnai1-derived clones (Figures 1a and b). Expression of EMT markers was then analysed. Re-expression of *E-cadherin* transcripts was detected in HaCa4 cells after double interference (HSS-C1/C7) to similar levels obtained after Snai1 silencing, but not in HaCa4-shSnai2 cells (Figure 1a, left), indicating that Snai1 expression is sufficient to repress *E-cadherin* in HaCa4 cells. No expression of E-cadherin protein could be detected in cultures of HaCa4-derived clones (Olmeda *et al*., 2007a; data not shown). Induction of *E-cadherin* expression could not be detected in CarB-derived clones (Figure 1a, right). The absence of genetic alterations in the *E-cadherin* locus in CarB cells (Navarro *et al*., 1991; Rodrigo *et al*., 1999), suggests that additional repressors or epigenetic mechanisms affect *E-cadherin* expression in this cell line; indeed, hypermethylation of *E-cadherin* promoter was detected in CarB cells (Fraga *et al*., 2004). Expression of the mesenchymal markers vimentin and fibronectin, was not affected by Snai2 silencing but was significantly decreased (50–60%) in double interfered CarB cells (CSS-D5/D10; Figure 1c, right), similar to CarB-shSnai1 cells (Olmeda *et al*., 2007a). Vimentin and fibronectin expression was moderately reduced in double interfered HaCa4 (HSS-C1/C7; 30–40%), but not affected in HaCa4-shSnai2 (Figure 1c, left) or HaCa4-shSnai1 cells (Olmeda *et al*., 2007a). These results, suggest that Snai1 and Snai2 can cooperate in the expression of mesenchymal markers in a cell context dependent manner. Silencing of Snai1 and/or Snai2 induces subtle changes in the epithelioid phenotype of HaCa4 cells that grow in compact epithelial-like islands at low cell density; however, at confluence the phenotype was not influenced (Supplementary Figure S2A, left panels). No changes in the spindle phenotype of CarB cells was detected after Snai1 and/or Snai2 knockdown at any density (Supplementary Figure S2B). In agreement with the morphological phenotype, Snai1 and/or Snai2 silencing did not modify the organization of the F-actin and microtubule cytoskeleton of either cell type (Supplementary Figures S2A and B).

We next analysed the effect of Snai2 and/or Snai1 silencing on MMP-9. Double interfered HaCa4 (HSS-C1/C7) and CarB (CSS-D5/D10) cells showed moderate to strong decrease in secreted MMP-9 activity (40–60%), to levels similar to those obtained after Snai1 silencing (Figure 2a). Interestingly, no changes or even increased MMP-9 activity was detected after Snai2 silencing in HaCa4 or CarB cells, respectively (Figure 2a). These results support a main role for Snai1 in the regulation of MMP-9, in agreement with the reported Snai1 upregulation of *MMP9* promoter (Jorda *et al*., 2005). In contrast, MMP-2 activity was not significantly affected by Snai1 and/or Snai2 silencing, although a slight increase was detected over controls in the HaCa4 system (Figure 2a, left). Finally, to analyse the biological effect of Snai1 and Snai2 silencing in invasion, transwell assays were performed. Snai2

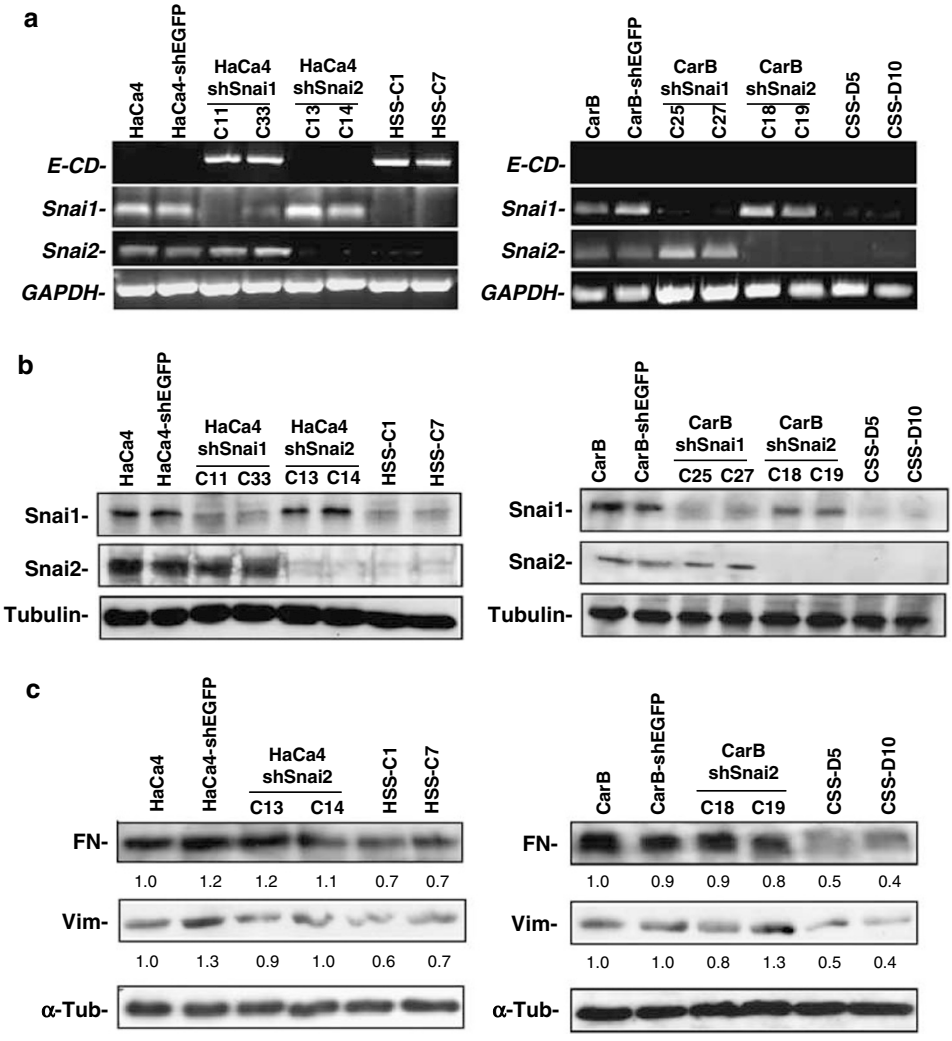

Figure 1 Characterization of HaCa4 and CarB derived clones after stable expression of shSnai2 and/or shSnai1 vectors. (**a**) Reverse transcription (RT)–PCR analysis of mouse *E-cadherin*, *Snai1* and *Snai2* transcripts in HaCa4 (left) and CarB (right) parental cells and the indicated stable clones obtained after expression of shSnai2 and/or shSnai1, or control shEGFP. *GADPH* levels are shown as loading control. (**b**; **c**) Western-blot analysis of (**b**) Snai1 and Snai2, and (**c**) fibronectin (FN) and vimentin (Vim) in the indicated cell lines. α-Tubulin (α-Tub) is shown as loading control. The relative values of FN and Vim expression, regarding α-Tub, are indicated for each cell line. Values obtained for parental HaCa4 and CarB cells were set to 1.0.

silencing induced a slight but significant reduction in the *in vitro* invasiveness of CarB cells (Figure 2b, right), whereas it did not affect invasion of HaCa4 cells (Figure 2b, left). In contrast, Snai1 silencing provokes a marked decrease in invasion in both cell types (Figure 2b). Importantly, further reduction was observed after Snai1/Snai2 silencing (Figure 2b), suggesting the active collaboration of both factors in induction of a fully invasive phenotype in HaCa4 and CarB cells.

Snai1 and Snai2 interference dramatically decreases tumor growth potential

Snai1 silencing in HaCa4 and CarB cells induces a strong reduction in xenograft growth rate and leads to more differentiated tumor phenotype (Olmeda *et al*., 2007a). To analyse if Snai1 and Snai2 collaborate on tumor growth and/or differentiation potential, two independent clones from each transfection type were orthotopically (subcutaneously) injected (1×10^6 cells per site) into nude mice, in parallel with the corresponding parental and control cells. All clones formed primary tumors at all injection sites. Tumors induced by HaCa4-shSnai2 and CarB-shSnai2 cells grew at lower rates than those induced by parental or control cells; about 30–40% reduction in tumor volume was observed in HaCa4-shSnai2 and CarB-shSnai2 xenografts at 14 and 17 days post-injection (d.p.i.), respectively (Figure 3a). Snai1 silencing induced a much stronger effect, particularly in HaCa4 cells, where a 90% reduction was observed 14 d.p.i. (Figure 3a, left). Notably, double Snai1/Snai2 interference induced a dramatic 95% tumor volume reduction of CarB-SS and further reduced, up to 99%, the tumor volume of HaCa4-SS xenografts at 17 and 14 d.p.i., respectively (Figure 3a). The strong reduction in the tumor growth potential induced by

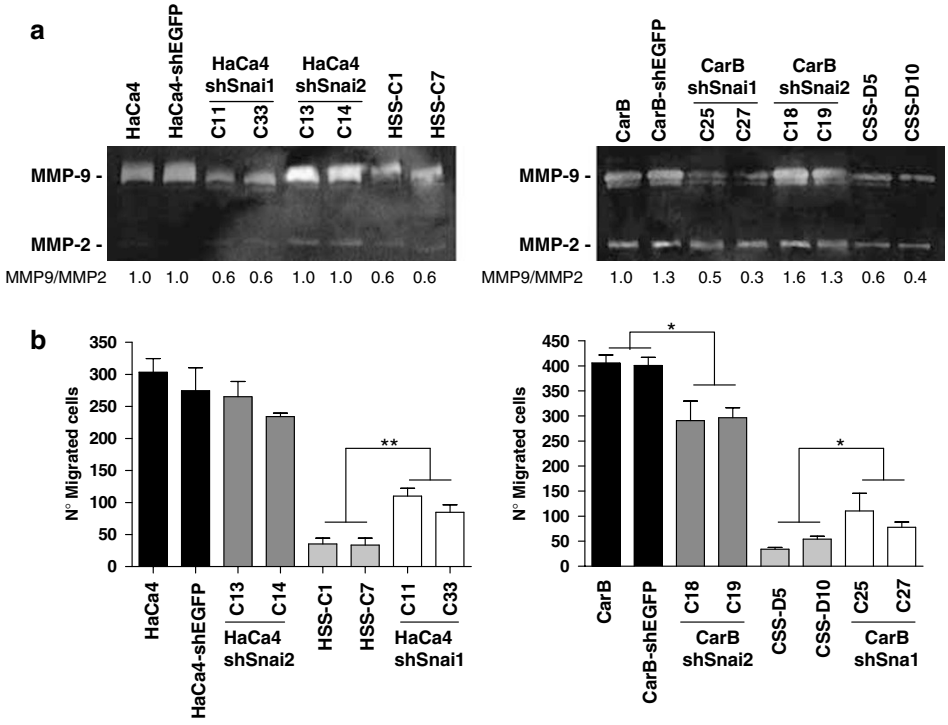

Figure 2 Analysis of MMP-9 activity and invasiveness of HaCa4 and CarB derived clones. (**a**) Zymography assays of MMP-9 secreted activity in conditioned media from HaCa4 (left) and CarB (right) parental cells and the indicated stable clones, or control shEGFP cells. MMP-2 activity is shown as control. A representative example of four independent assays is presented. The MMP9/MMP2 ratio is indicated for each cell line, compared to the ratio obtained in parental HaCa4 and CarB cells. (**b**) Analysis of the invasive phenotype of control cell lines and clones described in (a), performed in transwell filters coated with collagen type IV matrix. Cells into the lower chamber were counted 24 h after seeding. Results show the mean ± s.d. of three independent assays performed on duplicated samples. ANOVA analysis: $*P<0.05$; $**P<0.01$.

Snai1/Snai2 interference was maintained over time; HaCa4-SS and CarB-SS xenografts duplicate the latency period (time to reach 0.3 cm^3 volume; Figure 3a). A similar, although slightly faster, growth rate kinetics was detected in HaCa4- and CarB-shSnai1 xenografts. Similar results were obtained after subcutaneous injection of a lower number (1×10^5/site) of single and double interfered HaCa4 and CarB cells: under those conditions the latency period of control cells was almost duplicated (28 d.p.i.; Supplementary Figure S3). HaCa4- and CarB-shSnai1 cells exhibited increased latency (40–50 d.p.i.) that was further incremented in double interfered HaCa4-SS and CarB-SS cells (55–62 d.p.i; Supplementary Figure S3). A significant effect of Snai2 silencing was also detected in low cell injections in CarB-shSnai2 xenografts. Those experiments also confirmed the strong collaborative effect of Snai1 and Snai2 in the tumorigenicity of HaCa4 cells, as the incidence of tumors decreased up to 50% for HaCa4-SS cells (Supplementary Table S1), suggesting a role of Snai1/Snai2 in tumor cell maintenance. Together, these results indicate that Snai2 influences the tumorigenic behaviour of CarB cells, and collaborates with Snai1 on tumor growth potential of both HaCa4 and CarB cells.

RT–PCR and immunoblot analysis of xenografts indicated that Snai1 and/or Snai2 remained silenced in all tumors derived from shSnai1 and/or shSnai2 clones from HaCa4 or CarB cells (Figures 3b and c). Interestingly, re-expression of *E-cadherin* transcripts inside tumors was detected in those cases that maintained *Snai1*/*Snai2* silenced. Modest *E-cadherin* re-expression was also detected in HaCa4-shSnai2 xenografts (Figure 3b) and confirmed at protein level in HaCa4-shSnai1- and/or HaCa4-shSnai2-derived tumors, and CarB-SS xenografts by immunoblot (Figure 3c) and immunohistochemical analyses (see below). These results, therefore, indicate that Snai1/Snai2 silencing contributes to effectively de-repress E-cadherin in *in vivo* contexts.

Histological and immunofluorescence analysis of the xenografts confirmed the biological effect of Snai2 and/or Snai1 blockade. HaCa4-shEGFP and CarB-shEGFP cells induced tumors with histological characteristics similar to those induced by their corresponding controls, poorly differentiated squamous (Figures 4A, a and d) and spindle cell carcinoma (Figures 5A, a and d), respectively. Tumors induced by HaCa4-shSnai2 cells showed a moderately differentiated squamous cell phenotype (Figures 4A, b and e). Noteworthy, tumors induced by HSS-C1 cells showed a well-differentiated squamous cell phenotype with extensive areas of full keratinization (Figures 4A, c and f), a phenotype quite similar to that induced by HaCa4-shSnai1 cells (Olmeda *et al*., 2007a). In contrast, no significant changes were

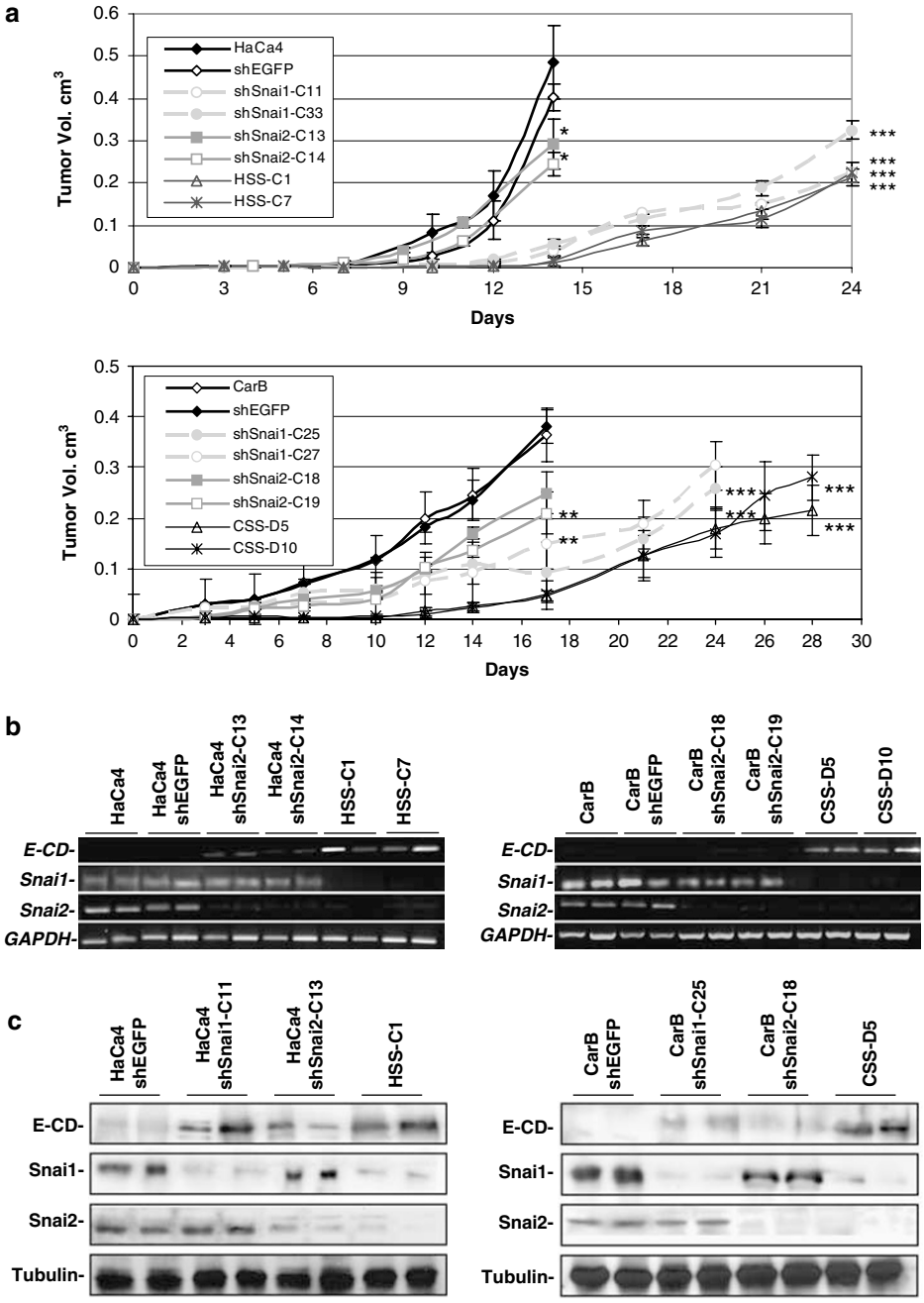

Figure 3 Silencing of Snai1 and Snai2 strongly decreases the tumorigenic potential of HaCa4 and CarB cells and leads to *in vivo* re-expression of E-cadherin. (**a**) The tumorigenic potential of HaCa4 (upper panel) and CarB (lower panel) cells and the indicated stable clones or control shEGFP cells was analysed by orthotopic subcutaneous injection into nude mice. Tumor growth was determined over the indicated time periods. Mice-bearing tumors from parental and shEGFP cells were killed at 14 (HaCa4) and 17 (CarB) days post injection. ANOVA analysis: $*P<0.05$; $**P<0.01$; $***P<0.001$. (**b**) Reverse transcription (RT)–PCR and (**c**) western blot analysis of Snai1, Snai2 and E-cadherin performed on (b) RNA and (c) protein extract samples isolated from two individual tumors generated by HaCa4 (left) or CarB (right) cells and the indicated derived clones. *GAPDH* mRNA and α-tubulin levels were included as loading control.

detected in the spindle phenotype of tumors induced by CarB-shSnai2 or CSS-D5 cells (Figures 5A, a–f). In agreement with the histological pattern, immunohistochemical analyses showed re-expression of E-cadherin at cell–cell contacts in HaCa4-shSnai2 and HSS-C1 xenografts, particularly at the most differentiated regions (Figures 4A, h and i). E-cadherin was also detected in CSS-D5, in a diffuse pattern (Figure 5A, i), in contrast to the total lack of E-cadherin in CarB-shEGFP and CarB-shSnai2 xenografts (Figures 5A, g and h). Cyclin D1 expression was markedly decreased in HaCa4-shSnai2 and HSS-C1 xenografts regarding control HaCa4-shEGFP tumors (Figures 4A, j–l); a similar situation was detected in CarB-derived tumors (Figure

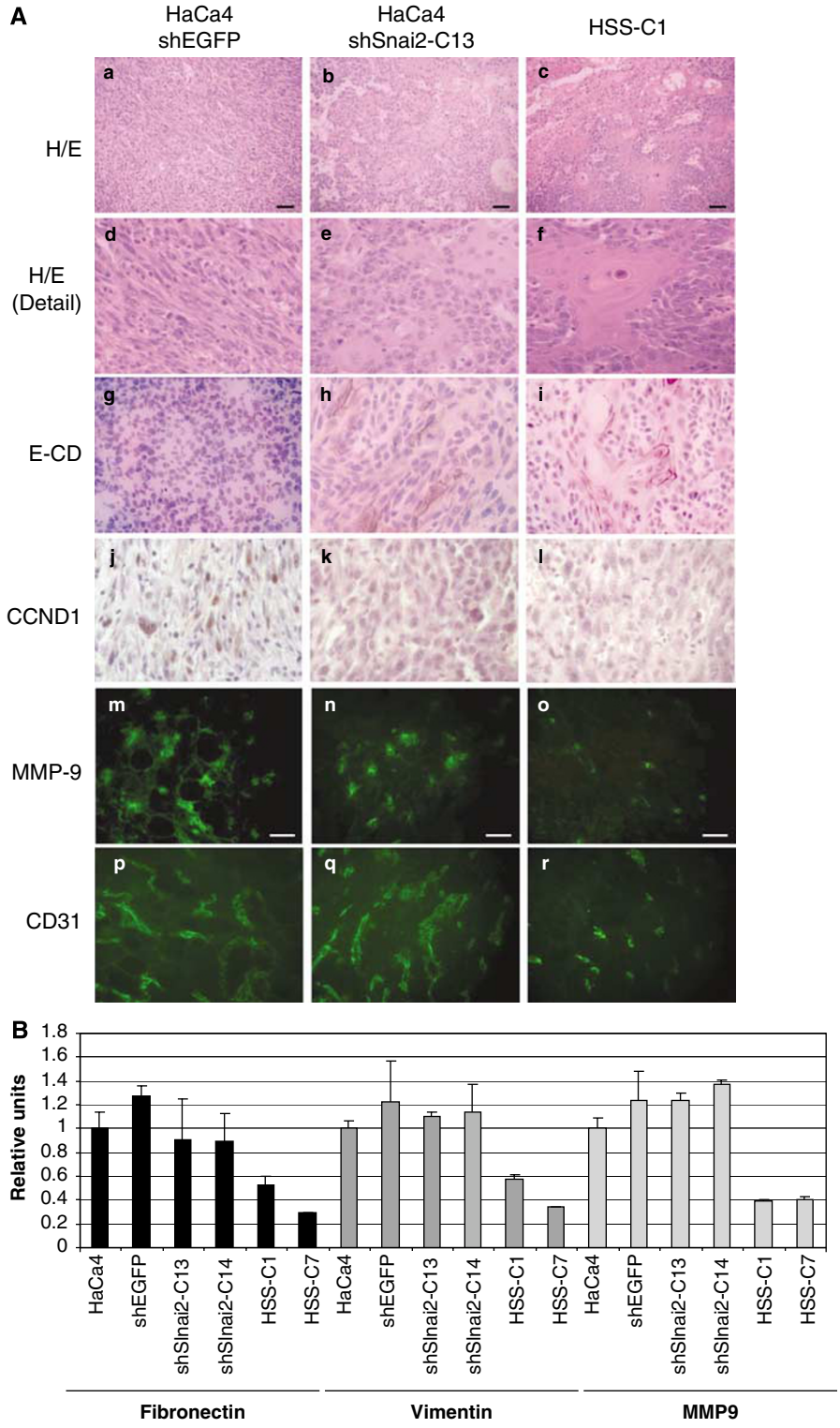

Figure 4 Silencing of Snai1 and Snai2 in HaCa4 cells induces tumors with more differentiated and lower invasive/angiogenic phenotype. (**A**) Histological and immunostaining analysis of tumors induced by representative HaCa4-derived clones after expression of shSnai2 (HaCa4shSnai2-C13), shSnai1 and shSnai2 (HSS-C1) or control shEGFP cells. (**a**–**c**) Low and (**d**–**f**) high power images of the histology of the indicated tumors. Immunohistochemical analyses of tumor sections for detection E-cadherin (E-CD) (**g**–**i**) and cyclin D1 (CCND1) (**j**–**l**). Immunofluorescence analyses of tumor sections for MMP-9 (**m**–**o**) and CD-31 (**p**–**r**) detection. Note the moderately (HaCa4-shSnai2-C13) and well-differentiated squamous carcinoma phenotype (HSS-C1) with abundant areas of keratinization and low cyclin D1 expression in the later. Bars, 50 μm. (**B**) Quantitative real-time (qRT)-PCR analyses of *fibronectin*, *vimentin* and *MMP-9* expression in the indicated HaCa4-derived tumors. The average values ± s.d. from two independent tumors per cell line are shown. Values were normalized to HaCa4 cells for each transcript.

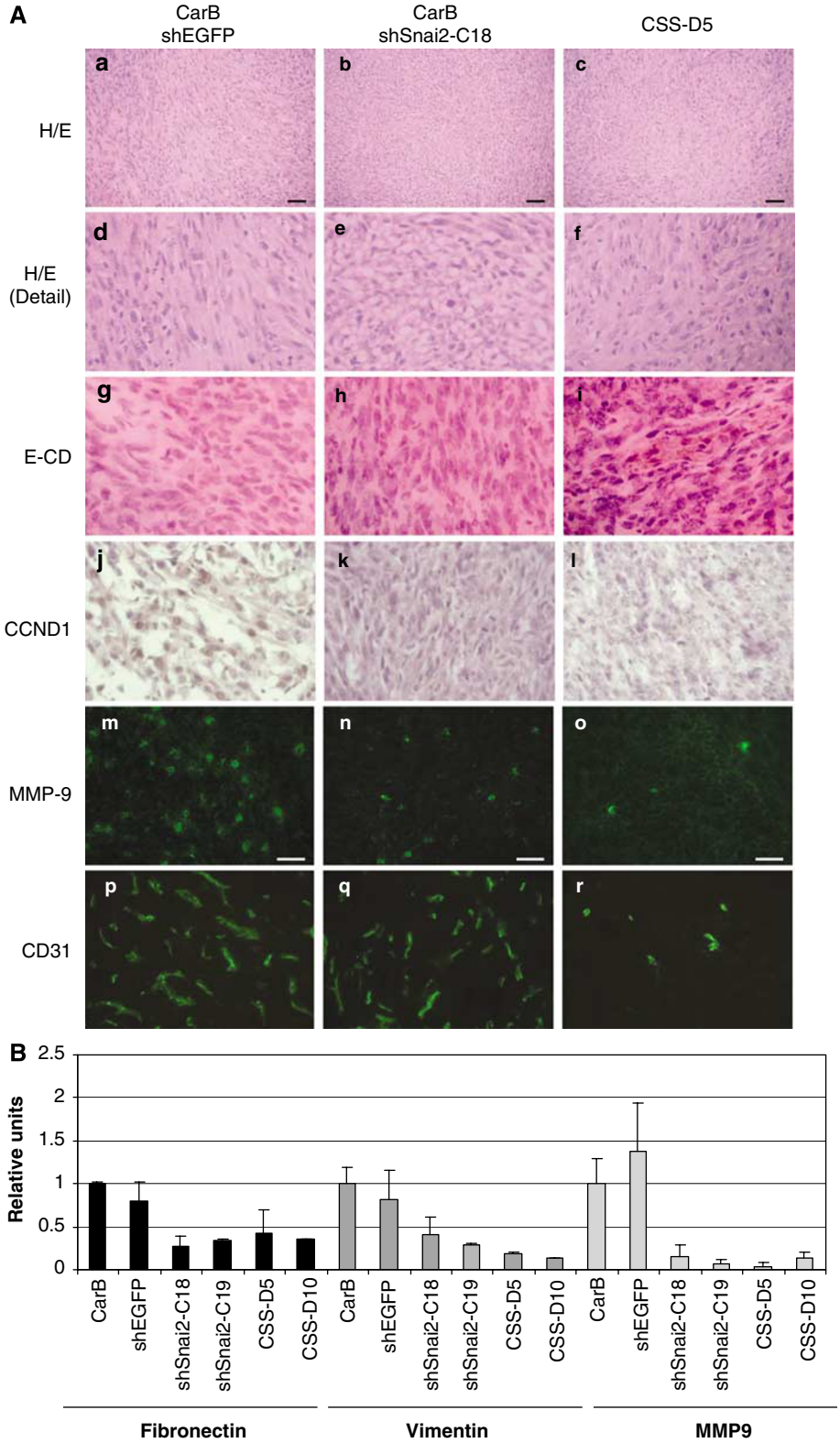

Figure 5 Silencing of Snai1 and Snai2 in CarB cells induces tumors with lower invasive/angiogenic phenotype. (**A**) Histological and immunostaining analysis of tumors induced by representative CarB-derived clones after expression of shSnai2 (CarBshSnai2-C18), shSnai1 and shSnai2 (CSS-D5) or control shEGFP cells. (**a**–**c**) Low and (**d**–**f**) high power images of the histology of the indicated tumors. Immunohistochemical analyses of tumor sections for detection E-cadherin (E-CD) (**g**–**i**) and cyclin D1 (CCND1) (**j**–**l**). Immunofluorescence analyses of tumor sections for MMP-9 (**m**–**o**) and CD-31 (**p**–**r**) detection. Note the decreased expression of cyclin D1 and MMP-9 in CarBshSnai2-C18 and CSS-D5 xenografts. Bars, 50 μm. (**B**) Quantitative real-time (qRT)-PCR analyses of *fibronectin, vimentin* and *MMP-9* expression in the indicated CarB-derived tumors. The average values ± s.d. from two independent tumors per cell line are shown. Values were normalized to CarB cells for each transcript.

Table 1 Latency of primary tumours and overall mice survival in spontaneous metastasis assays

	HaCa4-derived sh clones				
	shEGFP	*shSnail1-C11*	*shSnail1-C33*	*shSnail2-C13*	*shSnail2-C14*
Latency[a] (days)	18.4 ± 2.2	30.7 ± 4.6	33.2 ± 3.6	18.2 ± 2.05	17.4 ± 2.6
Survival after injection[b] (days)	35.8 ± 2.3	56.3 ± 2.3	55 ± 3.9	35.4 ± 4.3	31.8 ± 6.9

[a]Latency estimated as time (in days) required for primary tumours to reach a 0.4 cm^3 volume, when then were surgically removed. A total of 4–5 mice per cell line were injected. Average ± s.d. is presented.
[b]Overall survival of mice, estimated as days after orthotopic injection of cells. Average ± s.d. is presented.

5A, j–l), in accordance with the low proliferation potential of shSnai1/Snai2-tumors. No expression of p21 was detected in control or sh-derived xenografts from HaCa4 or CarB cells (data not shown). No significant differences in the apoptotic index or presence of necrotic regions in shSnail1 and/or shSnail2 xenografts and their corresponding controls could be detected (data not shown). The *in vitro* proliferation potential of HaCa4 and CarB derived clones was not affected regarding their corresponding parental or control cell lines (Supplementary Figure S4) and no signs of senescence were detected in any cell type in culture (not shown). Immunofluorescence analysis of MMP-9 indicated strong reduction in HSS-C1 (Figure 4A, o) and CSS-D5 (Figure 5A, o) xenografts compared to controls. Interestingly, significant reduction of MMP-9 was also detected in CarB-shSnail2 xenografts (Figure 5A, n), suggesting a differential regulation of MMP-9 between *in vivo* and *in vitro* situations. Quantitative real-time PCR (qRT-PCR) confirmed the reduction of *MMP-9* transcripts in HSS-C1/C7 (Figure 4B), CSS-D5/D10 and CarB-shSnai2-C18/C19 tumors (Figure 5B). Moreover, a strong reduction in transcript levels of *fibronectin* and *vimentin* was detected in HSS-C1/C7 (Figure 4B), CSS-D5/D10 and CarB-shSnai2 xenografts (Figure 5B), further confirming the induction of a more differentiated, less invasive tumor phenotype after Snai1 and/or Snai2 silencing. Finally, CD31 staining of the central region of HSS-C1/C7 and CSS-D5/D10 xenografts showed a dramatic decrease in angiogenic potential regarding tumors induced by control and shSnai2-derived cells (Figures 4A and 5A, compare panel r to p and q). Together, these data suggest that inhibition of tumor growth induced by Snai2 and/or Snai1 silencing can be mediated by a combination of action on the proliferation, differentiation/angiogenic properties of HaCa4 and CarB cells in *in vivo* contexts.

Snai1 and Snai2 interference dramatically reduces the metastatic capability of HaCa4 carcinoma cells

We next analysed the effect of Snai1 or Snai2 silencing on the metastatic properties of HaCa4 cells. Spontaneous metastasis assays were performed in HaCa4-shSnai1-C11/C33 and HaCa4-shSnai2-C13/C14 clones, in parallel with control HaCa4 and HaCa4-shEGFP cells. After orthotopic subcutaneous injection, tumors were surgically removed when they reached a volume of 0.4 cm^3 and mice were allowed to live until they become moribund. During the process, the presence of lung metastasis was analysed by non-invasive magnetic resonance imaging (MRI). Mice injected with HaCa4-shSnai1-C11/C33 cells survive longer (nearly two-fold increase in the post-injection survival period) than HaCa4-shSnai2-C13/C14 and HaCa4-shEGFP injected mice (Table 1). Parental HaCa4 and control HaCa4-shEGFP cells metastasized into lung, liver and spleen (Figure 6; Table 2) with multiple metastatic nodes in almost all injected mice at 25–35 d.p.i. Noteworthy, a strong reduction in the metastatic ability of HaCa4-shSnai1-C11/C33 cells was detected (Figure 6; Table 2). Macrometastasis to different organs was observed only in 25% of HaCa4-shSnai1-C11-injected mice, and not in HaCa4-shSnai1-C33-injected mice. A few micrometastasis foci were detected in liver and spleen of mice injected with HaCa4-shSnai1-C11/C33 cells (Table 2). Interestingly, although Snai2 interference in HaCa4 cells did not strongly affect tumor latency and mice survival (Table 1, Figure 3a), a total block of liver metastasis and strong (60–80%) reduction in lung metastasis was found, but no effect on spleen metastasis was detected (Figure 6 and Table 2). Taken together, these results indicate a strong influence of Snai1 and Snai2 in the generation of liver and lung metastasis and a more specific effect of Snai1 in spleen dissemination of HaCa4 cells.

Discussion

The Snail family factors, Snai1 and Snai2, are key regulators of EMT (Nieto, 2002) and important players of tumor invasion. In addition, they participate in other meaningful biological processes, like induction of cell movement and survival, also potentially contributing to other aspects of tumor progression (Barrallo-Gimeno and Nieto, 2005). An increasing number of studies have shown Snai1 and/or Snai2 expression in a variety of tumors (Peinado *et al*., 2007), but whether they play specific or redundant functions in tumor progression remains largely unknown. We have started to approach this issue targeting Snai1 and/or Snai2 by RNA interference in mouse skin carcinoma cell lines HaCa4 and CarB. Our recent studies indicated that Snai1 silencing in both cell lines induces a more differentiated, less invasive phenotype with a significant reduction in their tumorigenic capacity (Olmeda *et al*., 2007a). SNAI1 knockdown also dramatically affects tumor

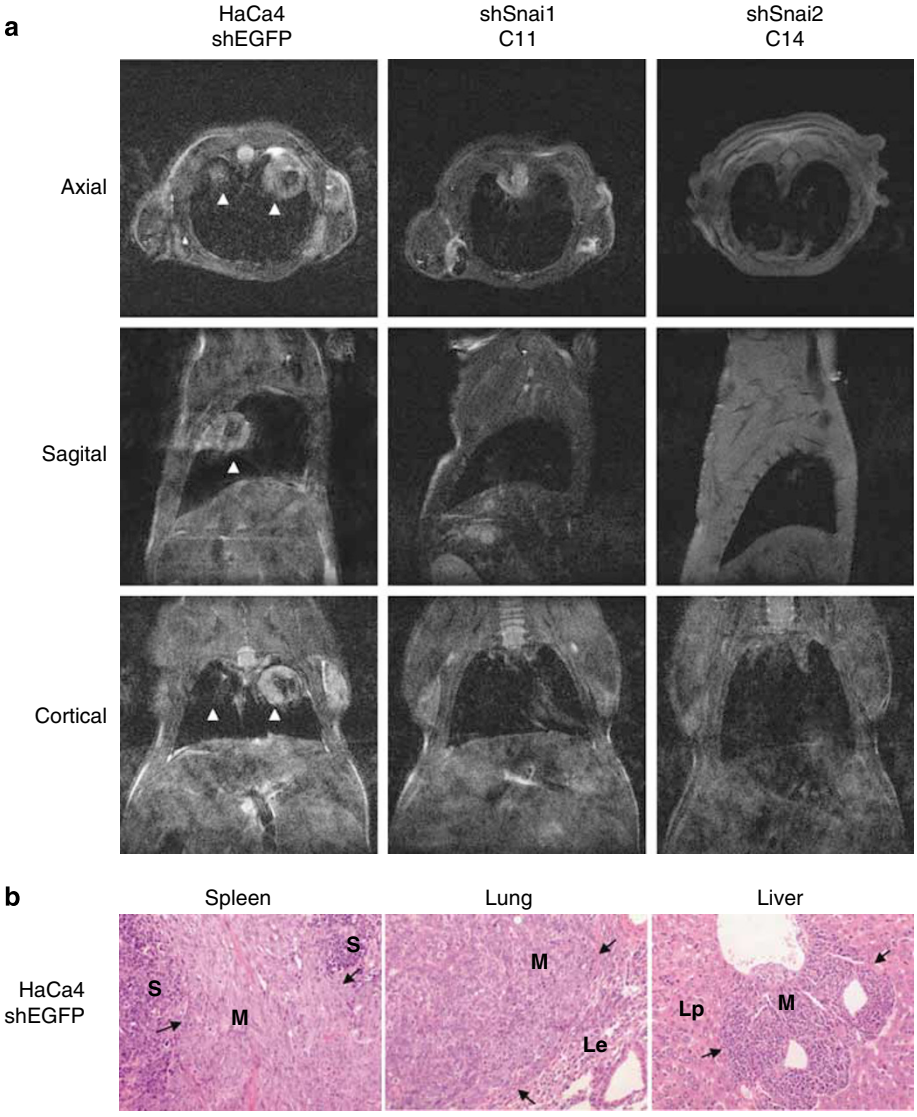

Figure 6 Snai1 or Snai2 silencing in HaCa4 cells abrogates lung metastasis. (**a**) T2 magnetic resonance imaging (MRI) pictures obtained from mice injected with the indicated HaCa4-derived clones after expression of shSnai1 (HaCa4shSnai1-C11), shSnai2 (HaCa4-shSnai2-C14) or control shEGFP cells. Axial, sagital and cortical images showing the lungs of representative mice, obtained at 25 (shEGFP, HaCa4shSnai2-C14) and 45 (HaCa4shSnai1-C11) days post-injection (d.p.i.) are presented. Arrowheads indicate the presence of metastasis. (**b**) Histological analysis of metastatic nodes from spleen, lung and liver of HaCa4-shEGFP injected mouse. Metastatic nodes (M) are delimited by arrows; S, spleen tissue; Le, lung epithelium; Lp, liver parenchyma.

Table 2 Metastasis generated in different organs by parental HaCa4 and sh derived clones

Cell line	*Metastasis*[a]			*Micrometastasis*[b]
	Spleen	*Lung*	*Liver*	
HaCa4	4/4	4/4	4/4	Lung, liver, spleen
HaCa4-shEGFP	3/5	5/5	3/5	Lung, liver, spleen
HaCa4-shSnail1-C11	1/4	1/4	1/4	Liver
HaCa4-shSnail1-C33	0/4	0/4	0/4	Liver, spleen
HaCa4-shSnail2-C13	5/5	2/5	0/5	Liver
HaCa4-shSnail2-C14	5/5	1/5	0/5	Liver

[a]Number of mice with macrometastatic nodules in the indicated organs per injected mice.
[b]Micrometastasis detected after microscopical inspection of the indicated organs.

growth and lymph node metastasis of human breast carcinoma cells (Olmeda *et al*., 2007b). We now report that Snai2 cooperates with Snai1 in tumor growth potential of HaCa4 and CarB and in the generation of lung and liver metastasis. An essential role for Snai1 in local invasion and tumor cell dissemination to spleen is also inferred from our present results.

In contrast to the effect observed after Snai1 silencing, Snai2 did not significantly modify the expression of *E-cadherin* or mesenchymal markers in HaCa4 or CarB cells when growing in culture, indicating that Snai1 is necessary and sufficient to repress *E-cadherin* and to maintain expression of mesenchymal markers *in vitro*. Vimentin/fibronectin upregulation by Snail factors are largely unknown but might involve indirect

transcriptional regulation (Guaita *et al*., 2002), as has been reported for Snai1 induction of *MMP9* and *ID1* genes (Jorda *et al*., 2005, 2007). The apparent higher potential of Snai1 over Snai2 in *E-cadherin* repression could be partly explained, by the higher affinity of Snai1 to the E-boxes of the *E-cadherin* promoter over Snai2 detected *in vitro* (Bolos *et al*., 2003) and supported by the expression of E-cadherin in Snai1−/Snai2+ mouse keratinocyte cell lines (Cano *et al*., 2000). Nevertheless, re-expression of E-cadherin was detected in HaCa4-shSnai2 and in CarB-SS xenografts, suggesting that Snai2 can also contribute to the full repression of *E-cadherin* in certain *in vivo* contexts. Apart from E-cadherin regulation, acquisition of well-differentiated squamous carcinoma phenotype seems to depend mainly on Snai1 silencing (Figure 4A; Olmeda *et al*., 2007a), supporting that Snai1 predominates over Snai2 in the maintenance of poorly differentiated squamous cell carcinoma phenotype.

Importantly, Snai1 expression is determinant for invasiveness, as Snai1 silencing significantly decreases *in vitro* invasion of HaCa4 and CarB cells, whereas Snai2 silencing only modestly affect CarB cells invasiveness. However, Snai2 appears to collaborate in the control of tumor invasion, as further reduction of invasion was observed in HaCa4 and CarB cells interfered for Snai1/Snai2 (Figure 2b). The collaboration of Snai2 in invasion appears to be independent of MMP9/MMP2 expression/activity suggesting that other methaloproteinases and/or proinvasive molecules could be regulated by Snai2. Nevertheless, a significant decrease of MMP9 and mesenchymal markers was detected in CarB-shSnai2 xenografts (Figure 5), suggesting that Snai2 can control certain aspects of tumor invasion/differentiation in determined tumor contexts. These observations are also compatible with the differential roles proposed for Snai1 and Snai2 factors in individual vs collective tumor invasion, or distinct anatomic dissemination of breast and ovarian tumors (Elloul *et al*., 2005, 2006; Come *et al*., 2006), and for Snai2 in wound healing migration (Savagner *et al*., 2005).

The tumorigenic and spontaneous metastasis assays performed after Snai2 and/or Snai1 silencing have added new important insights into the *in vivo* role of both factors. As previously reported (Olmeda *et al*., 2007a), Snai1 silencing dramatically reduces the tumor growth rate of HaCa4 and CarB cells, whereas Snai2 silencing has a lower effect on both kinds of xenografts (Figure 3a). Importantly, Snai1/Snai2 silencing further reduces tumor growth rate in mouse skin carcinoma cells. Noteworthy, the reduction in tumor growth potential after Snai1/Snai2 silencing was associated with decreased tumoral MMP9 expression and reduced angiogenesis. These results support that Snai1 and Snai2 collaborate in induction of tumor growth. Furthermore, Snai1 and Snai2 actively participate in the generation of distant metastasis. Snail1 silencing almost completely abrogated the capacity of HaCa4 cells to produce distant metastasis, whereas Snai2 silencing reduced liver, and to a lower extent, lung metastasis, but did not affect spleen metastasis. These differences in Snai1 and Snai2 action could reflect, at least in part, the different invasion potential induced by both factors. As such, the dramatic suppression of distant metastasis induced after Snai1 silencing could mainly be attributed to the strong blockade of local invasion, the first step of tumor metastasis. The lack of effect of Snai2 silencing in invasiveness and spleen metastasis also indicates that expression of Snai1 is sufficient to promote both local invasion and tumor cell dissemination into spleen. These results are also in line with the recent observation that SNAI1 expression is a requisite for lymph node metastasis of human breast carcinoma cells (Olmeda *et al*., 2007b). On the other hand, the strong influence of Snai2 silencing in reduction of liver and lung metastasis could be related to the cell survival properties (Inoue *et al*., 2002; Perez-Losada *et al*., 2003; Kajita *et al*., 2004) or the specific migration properties conferred by Snai2 (Barrallo-Gimeno and Nieto, 2005; Elloul *et al*., 2005; Come *et al*., 2006) that could restrain effective lung and liver colonization in its absence.

Taken together, the results presented here support that Snai1 and Snai2 collaborate on tumor growth potential and induction of distant metastasis, with complementary rather than redundant roles in tumor progression. Our results indicate that Snai1 is necessary for the onset of metastasis favouring local invasion, whereas Snai2 is additionally required for the establishment of distant site-specific lung and liver metastasis, supporting a sequential, hierarchical action of Snail factors during tumor progression of mouse skin carcinomas. Further studies are required to determine the collaboration of Snail factors in other tumor types.

Materials and methods

Generation of expression vectors and stable cell lines

Mouse CarB, HaCa4 and derived cell lines were grown as described (Olmeda *et al*., 2007a). The generation of shRNAs, against *EGFP* (shEGFP), or against mouse/human *Snai1* (shSnai1) have been described (Jorda *et al*., 2005). shRNA against mouse *Snai2* (5′-gctccactccactctcctt-3′; shSnai2) was generated by cloning into the pTER-Zeo vector. The different vectors were transfected using lipofectamine (Gibco BRL, San Diego, CA, USA), and stable transfectants obtained by selection with the appropriate antibiotic (1 μg/ml of puromycin and/or 100 μg/ml zeocyn) during 2–4 weeks. Clones (10–20) were isolated after each shRNA transfection and individually characterized, or collected as pooled clones in control transfections. The origin and characterization of HaCa4 and CarB cells has been previously described (Navarro *et al*., 1991; Llorens *et al*., 1998).

RT–PCR, quantitative RT-PCR and promoter analysis

Total RNA was isolated from the different cell lines and tumors, and RT–PCR carried out as described (Peinado *et al*., 2005). For qRT-PCR, cDNA was synthesized using High Capacity cDNA Archive Kit (Applied Biosystems, Foster City, CA, USA). Primers and PCR conditions were as described (Olmeda *et al*., 2007a). The proximal mouse *E-cadherin*-Luc (−178 to +92) promoter was used as described (Olmeda *et al*., 2007a).

Cell extracts and western blot analysis
Whole cell extracts were prepared and western blotting performed as described (Olmeda *et al*., 2007a). The primary antibodies used included: mouse monoclonal anti-α-tubulin (1:1000; Sigma Chemical Co., St Louis, MO, USA) and anti-vimentin (1:2000; Babco, Emeryville, CA, USA), rat monoclonal anti-E-cadherin (ECCD-2; 1:200) and rabbit polyclonal anti-fibronectin (1:4000; Sigma Chemical Co.).

Gelatin zymography and invasion assays
Gelatin zymography was performed essentially as described (Jorda *et al*., 2005). Invasion assays were performed on modified Boyden chambers (0.8 μm pore) coated with collagen type IV gel as described (Olmeda *et al*., 2007a).

Local tumor growth and spontaneous metastasis
For tumorigenic analysis, cells from subconfluent cultures were orthotopically (subcutaneous) injected (1×10^6 or 1×10^5 in 0.1 ml phosphate buffered saline (PBS)) into the two flanks of 8-week female Balb/c nude mice (Charles River, Wilmington, MA, USA). Growing tumors were measured every two days using caliper by determination of the two orthogonal external diameters. Mice were killed when tumors reached 0.5 cm^3 size; tumors were surgically excised and processed for histology, immunofluorescence and RT–PCR analysis as described (Peinado *et al*., 2005). A minimum of eight tumors per cell line were generated and, at least, four different tumors from each cell line were analysed.

For spontaneous metastasis assay, cells from subconfluent cultures were orthotopically injected (1×10^6 in 0.1 ml PBS) into the dorsal midline of female Balb/c nude mice. Tumors were surgically removed when they reached 0.4 cm^3 size. Development of lung metastasis was followed thereafter by MRI. Mice were killed when they become moribund or after a maximum of 60 d.p.i. Four to five mice were injected per cell line. Mice were housed and maintained under specific pathogen-free conditions and used in accordance with institutional guidelines and approved by the Use Committee for Animal Care.

Magnetic resonance imaging
Magnetic resonance images were acquired on a Bruker Pharmascan 7 Tesla platform (Bruker Biospin, Ettlingen, DE, USA) using a 3.8 mm whole body rodent resonator. Animals were anaesthetized with 1% isofluorane/oxygen mixture and the temperature maintained in the physiological range through a circulating water pad. Axial, sagital and cortical slices (1 mm) were acquired from the upper thorax with T2 weighting (TR: 2500 ms, TE: 59.1 ms), using a 256×192 pixel matrix through the complete field of view. Images were processed using the Bruker Paravision 4.0 program.

Histological, immunohistochemical, RT–PCR, western blots and tunel analyses of primary tumors
Histology on paraffin tumor sections and immunostaining of frozen section with anti-E-cadherin, anti-MMP-9 and anti-CD31 was performed as described (Olmeda *et al*., 2007a). Immunostaining for cyclin D1 was performed on paraffin sections with rabbit anti-cyclin D1 (1:100; Neo Markers, Fremont, CA, USA), as previously described (Moreno-Bueno *et al*., 2003). RT–PCRs, western blot analyses and tunel assays on frozen tumor sections were carried out as described (Peinado *et al*., 2005).

Statistical analysis
All statistical comparisons were made using the analysis of variance (ANOVA) analysis.

Abbreviations

d.p.i., days post-injection; EMT, epithelial-mesenchymal transition; MDCK, Madin Darby canine kidney; MMP, metalloproteinase; MRI, magnetic resonance imaging; qRT-PCR, quantitative real-time PCR; RT–PCR, reverse transcription–PCR; shRNA, small hairpin interfering RNA.

Acknowledgements

We thank Vanesa Santos for excellent technical assistance, P López for MRI analysis, H Clevers for the pTER-Zeo vector and H Peinado for critical reading of the article. This work was supported by grants from the Spanish Ministry of Education and Science (SAF2004-00361; SAF2007-63051; NAN2004-09230-C04-02; Consolider-Ingenio CSD00C-2007-26102) and the EU (MRTN-CT-2004-005428).

References

Barrallo-Gimeno A, Nieto MA. (2005). The Snail genes as inducers of cell movement and survival: implications in development and cancer. *Development* **132**: 3151–3161.

Batlle E, Sancho E, Franci C, Dominguez D, Monfar M, Baulida J *et al*. (2000). The transcription factor snail is a repressor of E-cadherin gene expression in epithelial tumor cells. *Nat Cell Biol* **2**: 84–89.

Birchmeier W, Behrens J. (1994). Cadherin expression in carcinomas: role in the formation of cell junctions and the prevention of invasiveness. *Biochim Biophys Acta* **1198**: 11–26.

Bolos V, Peinado H, Perez-Moreno MA, Fraga MF, Esteller M, Cano A. (2003). The transcription factor Slug represses E-cadherin expression and induces epithelial to mesenchymal transitions: a comparison with Snail and E47 repressors. *J Cell Sci* **116**: 499–511.

Cano A, Perez-Moreno MA, Rodrigo I, Locascio A, Blanco MJ, del Barrio MG *et al*. (2000). The transcription factor snail controls epithelial-mesenchymal transitions by repressing E-cadherin expression. *Nat Cell Biol* **2**: 76–83.

Carver EA, Jiang R, Lan Y, Oram KF, Gridley T. (2001). The mouse snail gene encodes a key regulator of the epithelial-mesenchymal transition. *Mol Cell Biol* **21**: 8184–8188.

Christofori G. (2006). New signals from the invasive front. *Nature* **441**: 444–450.

Christofori G, Semb H. (1999). The role of the cell-adhesion molecule E-cadherin as a tumor-suppressor gene. *Trends Biochem Sci* **24**: 73–76.

Come C, Magnino F, Bibeau F, De Santa Barbara P, Becker KF, Theillet C *et al*. (2006). Snail and slug play distinct roles during breast carcinoma progression. *Clin Cancer Res* **12**: 5395–5402.

Elloul S, Elstrand MB, Nesland JM, Trope CG, Kvalheim G, Goldberg I *et al*. (2005). Snail, Slug, and Smad-interacting protein 1 as novel parameters of disease aggressiveness in metastatic ovarian and breast carcinoma. *Cancer* **103**: 1631–1643.

Elloul S, Silins I, Trope CG, Benshushan A, Davidson B, Reich R. (2006). Expression of E-cadherin transcriptional regulators in ovarian carcinoma. *Virchows Arch* **449**: 520–528.

Fraga MF, Herranz M, Espada J, Ballestar E, Paz MF, Ropero S *et al*. (2004). A mouse skin multistage carcinogenesis model reflects the aberrant DNA methylation patterns of human tumors. *Cancer Res* **64**: 5227–5234.

Guaita S, Puig I, Franci C, Garrido M, Dominguez D, Batlle E *et al*. (2002). Snail induction of epithelial to mesenchymal transition in tumor cells is accompanied by MUC1 repression and ZEB1 expression. *J Biol Chem* **277**: 39209–39216.

Gupta GP, Massague J. (2006). Cancer metastasis: building a framework. *Cell* **127**: 679–695.

Hajra KM, Chen DY, Fearon ER. (2002). The SLUG zinc-finger protein represses E-cadherin in breast cancer. *Cancer Res* **62**: 1613–1618.

Inoue A, Seidel MG, Wu W, Kamizono S, Ferrando AA, Bronson RT *et al*. (2002). Slug, a highly conserved zinc finger transcriptional repressor, protects hematopoietic progenitor cells from radiation-induced apoptosis *in vivo*. *Cancer Cell* **2**: 279–288.

Jiang R, Lan Y, Norton CR, Sundberg JP, Gridley T. (1998). The Slug gene is not essential for mesoderm or neural crest development in mice. *Dev Biol* **198**: 277–285.

Jorda M, Marazuela E, Vinyals A, Cubillo E, Olmeda D, Valero E *et al*. (2007). Id-1 is induced in MDCK epithelial cells by activated Erk/MAPK pathway in response to expression of the Snail and E47 transcription factors. *Exp Cell Res* **313**: 2389–2403.

Jorda M, Olmeda D, Vinyals A, Valero E, Cubillo E, Llorens A *et al*. (2005). Upregulation of MMP-9 in MDCK epithelial cell line in response to expression of the Snail transcription factor. *J Cell Sci* **118**: 3371–3385.

Kajita M, McClinic KN, Wade PA. (2004). Aberrant expression of the transcription factors snail and slug alters the response to genotoxic stress. *Mol Cell Biol* **24**: 7559–7566.

Llorens A, Rodrigo I, Lopez-Barcons L, Gonzalez-Garrigues M, Lozano E, Vinyals A *et al*. (1998). Down-regulation of E-cadherin in mouse skin carcinoma cells enhances a migratory and invasive phenotype linked to matrix metalloproteinase-9 gelatinase expression. *Lab Invest* **78**: 1131–1142.

Manzanares M, Locascio A, Nieto MA. (2001). The increasing complexity of the Snail gene superfamily in metazoan evolution. *Trends Genet* **17**: 178–181.

Mehlen P, Puisieux A. (2006). Metastasis: a question of life or death. *Nat Rev Cancer* **6**: 449–458.

Moreno-Bueno G, Rodríguez-Perales S, Sánchez-Estévez C, Hardisson D, Sarrió D, Prat J *et al*. (2003). Cyclin D1 gene (*CCND1*) mutations in endometrial cancer. *Oncogene* **22**: 6115–6118.

Navarro P, Gomez M, Pizarro A, Gamallo C, Quintanilla M, Cano A. (1991). A role for the E-cadherin cell-cell adhesion molecule during tumor progression of mouse epidermal carcinogenesis. *J Cell Biol* **115**: 517–533.

Nieto MA. (2002). The snail superfamily of zinc-finger transcription factors. *Nat Rev Mol Cell Biol* **3**: 155–166.

Olmeda D, Jorda M, Peinado H, Fabra A, Cano A. (2007a). Snail silencing effectively suppresses tumor growth and invasiveness. *Oncogene* **26**: 1862–1874.

Olmeda D, Moreno-Bueno G, Flores JM, Fabra A, Portillo F, Cano A. (2007b). SNAI1 is required for tumor growth and lymph node metastasis of human breast carcinoma MDA-MB-231 cells. *Cancer Res* **67**: 11721–11731.

Peinado H, Iglesias-de la Cruz MC, Olmeda D, Csiszar K, Fong KS, Vega S *et al*. (2005). A molecular role for lysyl oxidase-like 2 enzyme in snail regulation and tumor progression. *EMBO J* **24**: 3446–3458.

Peinado H, Olmeda D, Cano A. (2007). Snail, Zeb and bHLH factors in tumor progression: an alliance against the epithelial phenotype? *Nat Rev Cancer* **7**: 415–428.

Perez-Losada J, Sanchez-Martin M, Perez-Caro M, Perez-Mancera PA, Sanchez-Garcia I. (2003). The radioresistance biological function of the SCF/kit signaling pathway is mediated by the zinc-finger transcription factor Slug. *Oncogene* **22**: 4205–4211.

Rodrigo I, Cato AA, Cano A. (1999). Regulation of E-cadherin gene expression during tumor progression: the role of a new Ets-binding site and the E-pal element. *Exp Cell Res* **248**: 358–371.

Savagner P, Kusewitt DF, Carver EA, Magnino F, Choi C, Gridley T *et al*. (2005). Developmental transcription factor slug is required for effective re-epithelialization by adult keratinocytes. *J Cell Physiol* **202**: 858–866.

Thiery JP. (2002). Epithelial-mesenchymal transitions in tumor progression. *Nat Rev Cancer* **2**: 442–454.

Supplementary Information accompanies the paper on the Oncogene website (http://www.nature.com/onc).